K^--Nucleus Scattering at Low and Intermediate Energies.

C. García-Recio,[1] A.J. Melgarejo,[1] and J.Nieves[1]

[1]*Departamento de Física Moderna, Universidad de Granada, E-18071 Granada, Spain*

We calculate K^--nucleus elastic differential, reaction and total cross sections for different nuclei (^{12}C,^{40}Ca and ^{208}Pb) at several laboratory antikaon momenta, ranging from 127 MeV to 800 MeV. We use different antikaon-nucleus optical potentials, some of them fitted to kaonic atom data, and study the sensitivity of the cross sections to the considered antikaon-nucleus dynamics.

PACS numbers: 13.75.Jz, 21.65.+f, 36.10.-k, 13.75.-n, 13.85.Dz,11.30.Rd

I. INTRODUCTION

The works on meson baryon dynamics of Ref. [1] showed how Chiral symmetry constraints could be accommodated within a unitarity approach, able to describe resonances. This proved to be crucial to disentangle the intricate interaction between antikaons and nucleons at low energies [2]–[4]. The model of Ref. [2], was employed in Ref. [5] to microscopically derive an optical potential for the K^- in nuclear matter in a self-consistent manner. Self-consistency turned out to be a crucial ingredient to derive the K^--nucleus potential and led to an optical potential considerably more shallow than those found in Refs. [6]–[8].

In Refs. [9] and [10], the predictions of the chirally inspired potential of Ref. [5] for measured shifts and widths of K^- atoms were evaluated, and it was found that this potential provides an acceptable description of the observed kaonic atom states, through the whole periodic table. Despite of having both real and imaginary parts of quite different depth, some other empirical optical potentials ([7]–[8]) also examined in Ref. [10], led to acceptable descriptions of the experimentally available K^- atom data as well. However, there were appreciable differences among the predicted widths for deeply bound antikaon nuclear states, not detected yet, when different potentials were used. The aim of this paper is to explore the possibility of differentiating between several K^- nucleus optical potentials by means of the scattering data. The extrapolation to finite K^- kinetic energies of the potential of Ref. [5] requires at least the inclusion of the p-wave part of the K^- selfenergy. This was performed in Ref. [11], and tested for K^-p scattering in Ref. [12]. However, even after having included p-wave contributions, one cannot expect reliable predictions from the theoretical potential of Refs. [5] and [11], at the lowest energy for which there exist experimental data (800 MeV for the K^- momentum), where d and f waves contributions are relevant. Besides, as we will show, for this relatively high energy, the impulse approximation works reasonably well, which is a clear indication that these data do not have much information on the details of the K^--nucleus dynamics. Thus, we have also focused our attention at the typical momentum of the K^- after the ϕ-meson decay ($\approx$ 127 MeV) with the hope that the scattering experience could be performed at DAΦNE or at KEK or in the future Japanese Hadron Collider (JHC).

II. K^--NUCLEUS OPTICAL POTENTIALS

We solve the Klein Gordon equation

$$\left(-\vec{\nabla}^2 + \mu^2 + 2\omega V_{\rm opt}\right)\Psi = \left(\omega - V_C\right)^2\Psi, \qquad (1)$$

where ω is the Center of Mass (CM) K^-–nucleus energy, V_C and $V_{\rm opt}$ are the finite-size Coulomb and optical K^-–nucleus potentials and μ the reduced K^--nucleus mass. At large distances and for a CM scattering angle θ, the K^- wave-function $\Psi(\vec{r})$ behaves as $I(r) + f(\theta)S(r)$, with $I(r)$ and $S(r)$ the standard wave functions for Coulomb scattering from a punctual charge Z and $f(\theta)$ the scattering amplitude, which normalization is determined by its relation to the CM differential elastic cross section $d\sigma_{\rm e}/d\Omega = |f(\theta)|^2$. The integrated cross sections read:

$$\sigma_{\rm e} = \frac{\pi}{q^2}\sum_l (2l+1)\left|1 - \eta_l e^{2{\rm i}\,(\sigma_l+\delta_l)}\right|^2, \qquad (2)$$

$$\sigma_{\rm t} = \frac{2\pi}{q^2}\sum_l (2l+1)\left[1 - \eta_l\cos\left(2\left(\sigma_l+\delta_l\right)\right)\right], \qquad (3)$$

$$\sigma_{\rm re} = \frac{\pi}{q^2}\sum_l (2l+1)\left[1 - \eta_l^2\right] \qquad (4)$$

with q the CM K^- momentum and σ_l, δ_l and η_l the standard Coulomb phase shifts, the additional phase shifts due to strong interaction and the inelasticities appearing in the standard partial wave decomposition of $f(\theta)$ (see Ref. [13]). While the elastic ($\sigma_{\rm e}$) and total ($\sigma_{\rm t}$) cross sections are infinite, the reaction ($\sigma_{\rm re}$) cross section is finite because of the short-range of the nuclear interaction.

The K^--nucleus optical potential, $V_{\rm opt}$, is related to the K^--selfenergy, $\Pi(q^0, |\vec{q}\,|)$, inside of a nuclear medium, neglecting isovector effects, by

$$2\omega V_{\rm opt}(r) = \Pi\left(m + T,\ ({q^0}^2 - m^2)^{\frac{1}{2}};\ \rho(r)\right) \qquad (5)$$

where m and T are the K^- mass and laboratory kinetic energy and ρ is the sum of proton and neutron densities.

From the antikaon-selfenergy, as determined by, Refs. [5] and [11], we define the first selfenergy used in this work ($\Pi^{\rm TH}$). This selfenergy does not have any free parameters, all the needed input is fixed either from studies of meson-baryon scattering in the vacuum or from previous studies of pion-nucleus dynamics [13]. It provides an acceptable (χ^2/dof of 2.9) description of the set of 63 shifts and widths of K^- atom levels used in Ref. [10]. We have neglected all type of non-localities, since they lead to changes in the results presented here of 3% at most.

As in Ref. [10], we also construct a modified selfenergy, which we call $\Pi^{\rm THPH}$, by adding to $\Pi^{\rm TH}$ a phenomenological part linear in density. This phenomenological part is determined by a constant δb_0 which we fix to the value $(0.12 - {\rm i}\ 0.38)$fm, obtained in Ref. [10] from a χ^2-fit to the kaonic atom data. The new selfenergy reads:

$$\Pi^{\rm THPH}(r) \;=\; \Pi^{\rm TH}(r) - 4\pi\ \delta b_0\ \rho(r) \qquad (6)$$

The third selfenergy considered in this work is just obtained from the Impulse Approximation (IA), i.e., $t\rho$ form for the K^- selfenergy, and it neglects all orders higher than the leading one, in the density expansion. It reads:

$$\Pi^{\rm IA}(r) \;=\; -4\pi\frac{\sqrt{s}}{M}\ b_0^{\rm IA}(\sqrt{s}\ )\rho(r) \qquad (7)$$

with $b_0^{\rm IA}(\sqrt{s}\ ) = \frac{1}{4}(3\ {}_1f(\sqrt{s}\ ) + {}_0f(\sqrt{s}\ ))$, M the nucleon mass, $\sqrt{s}$ the total CM K^-N energy and ${}_{I=1,0}f$ the isoscalar and isovector forward antikaon-nucleon scattering amplitudes, which partial wave decomposition reads:

$${}_If(\sqrt{s}\ ) = \sum_l \left((l+1)\ {}_If_l^{j_+}(\sqrt{s}\ ) + l\ {}_If_l^{j_-}(\sqrt{s}\ )\right) \qquad (8)$$

with $j_\pm = l \pm 1/2$ the total angular momentum. At threshold, $b_0^{\rm IA_{thr}} \equiv b_0^{\rm IA}(m+M) = (-0.15+{\rm i}\ 0.62)$ fm [14]. The IA leads to extremely poor results for kaonic atoms [6],[10]. This is a clear indication that higher density corrections, not taken into account within the IA, are extremely important for kaonic atoms.

Finally, we have also considered two other antikaon selfenergies fitted to the kaonic atom data and energy independent ([7] and [8]):

$$\Pi^{\rm 2DD} \;=\; -4\pi\left(1+\frac{\mu}{M}\right)\left(b_0^{\rm IA_{thr}} + B_0\left(\frac{\rho}{\rho_0}\right)^\alpha\right)\rho \qquad (9)$$

$$\Pi^{\rm IAPH} \;=\; -4\pi\left(1+\frac{\mu}{M}\right)\tilde{b}_0\rho \qquad (10)$$

with $\tilde{b}_0 = (0.52+{\rm i}\ 0.80)$ fm, $B_0 = (1.62-{\rm i}\ 0.028)$ fm and $\alpha = 0.273$ as determined from χ^2-fits to K^--atom data in Ref. [10]. Note that, though both $\Pi^{\rm IAPH}$ and $\Pi^{\rm IA}$ are linear in density selfenergies, they lead to substantially different potentials, since the real parts of the coefficients $\tilde{b}_0$ and $b_0^{\rm IA_{thr}}$ differ both in sign and in size.

III. RESULTS AND CONCLUDING REMARKS

Since the K^- lifetime is relatively small, in practical terms it is experimentally difficult to count with low energetic K^- beams. However, all selfenergies described in the previous section, except for that obtained in the IA, are valid only near threshold. Thus, we have studied the case $q_{\rm lab} = 127$ MeV, since this is the K^- momentum after the ϕ-meson decay. In Fig. 1 we present results obtained with the K^- selfenergies fitted to the kaonic atom data. We also show results obtained by using the IA, where we have approximated the IA selfenergy at $q_{\rm lab} = 127$ MeV by its threshold value quoted above. Strong interaction integrated elastic, reaction and total cross sections are also given in the top part of Table I. We obtain these cross sections after having got rid of the Coulombian interaction, otherwise the total and elastic cross sections would diverge, i.e., we compute strong phase-shifts and inelasticities (δ_l and η_l) in presence of the Coulomb interaction, and afterwards we set to zero the Coulombian phase shifts, σ_l, in the formulae of Eqs. (2)-(4). As can be seen in the figure,

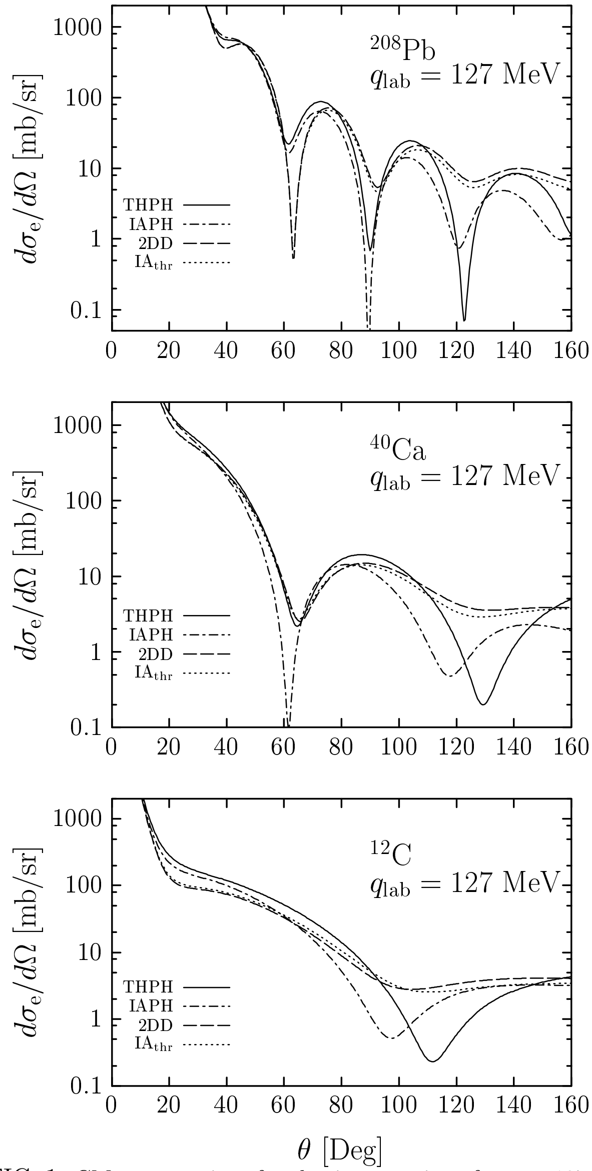

FIG. 1: CM cross sections for elastic scattering of $q_{\rm lab} = 127$ MeV K^- from ^{12}C, ^{40}Ca and ^{208}Pb with different K^- selfenergies.

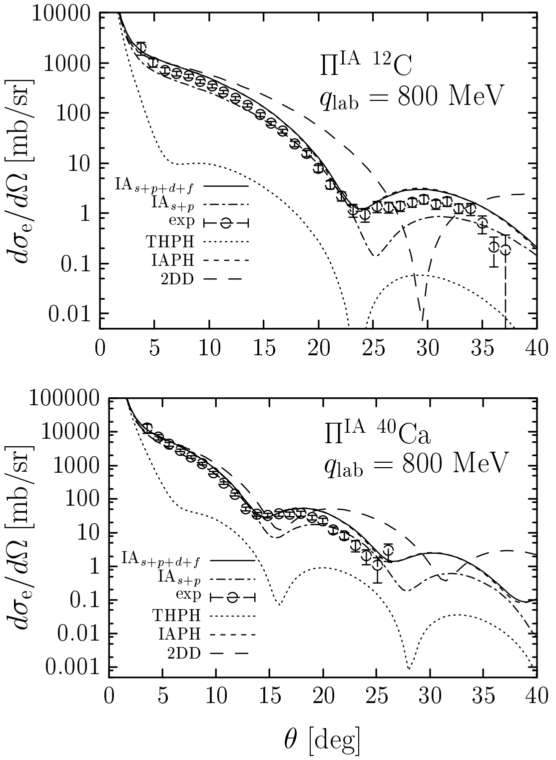

FIG. 2: CM differential cross section for elastic scattering of $q_{\mathrm{lab}} =$ 800 MeV K^- from ^{12}C and ^{40}Ca. Data are taken from Ref. [15].

	^{12}C			^{40}Ca			^{208}Pb		
Potential	σ_{e}	σ_{re}	σ_{t}	σ_{e}	σ_{re}	σ_{t}	σ_{e}	σ_{re}	σ_{t}
Π^{THPH}	444	501	945	1190	1201	2391	4345	4219	8564
Π^{2DD}	370	415	785	1064	1024	2088	4287	3667	7954
Π^{IAPH}	411	568	979	1029	1313	2342	4094	4363	8457
$\Pi^{\mathrm{IA}}\|_{\sqrt{s}=m+M}$	380	420	800	1040	1043	2083	4264	3699	7963
Π^{THPH}	71	250	321	242	572	814	1329	2074	3403
Π^{2DD}	252	312	564	545	737	1282	2057	2288	4345
Π^{IAPH}	250	374	624	613	858	1471	2115	2562	4677
$\Pi^{\mathrm{IA}}\|_{s+p}$	248	384	632	615	874	1489	2148	2557	4705
$\Pi^{\mathrm{IA}}\|_{s+p+d}$	278	406	684	653	913	1566	2195	2642	4837

TABLE I: Strong integrated elastic, reaction and total cross sections (in mb) at $q_{\mathrm{lab}} = 127$ (top) and 300 (bottom) MeV.

the non-linear density dependent K^- selfenergy, Π^{2DD}, and the linear density dependent, threshold IA selfenergy, $\Pi(\sqrt{s}\,) = \Pi^{\mathrm{IA}}|_{\sqrt{s}=m+M}$, provide extraordinarily similar results. Since both models have the same linear term in density, this is a clear indication that the reaction takes place in the surface of the nuclei, because of the big imaginary part of the potentials. The semiphenomenological Π^{THPH} selfenergy, has a stronger departure from a linear behaviour in density than Π^{2DD}, it has a smaller imaginary part (see Fig. 1 of Ref. [10]) and all of these explain the bigger differences with the IA model. Results, in particular position of the minima, obtained with Π^{THPH} are clearly distinguishable from those obtained with any of the other three models also plotted in the figure, pointing out to a clear different density behavior likely due to the selfconsistent derivation of it. As a matter of example, for ^{12}C in the region around $\theta = 60^{\mathrm{o}}$, 2DD, IA and IAPH give similar elastic cross sections of about 33 mb/sr, whereas THPH gives about 52 mb/sr. This difference is appreciable and the size of the cross sections, tens of mb/sr, might allow to measure such a difference at DAΦNE or KEK or in the future at the JHC. The differences are even bigger for larger angles, around the minimum of the THPH cross section (region 110-130$^{\mathrm{o}}$), but there, the cross sections are smaller, which makes harder to get the required statistics to see the effect. Besides, theoretical results in the neighborhood of a minimum are subject to more uncertainties. Similar conclusions can be drawn from the ^{40}Ca and ^{208}Pb results. In what respects to the integrated cross sections of Table I, 2DD and IA give similar cross sections, though the IA reaction cross section is always slightly bigger, because the imaginary part of the B_0 parameter in Eq. (9) is negative. The IAPH model always provides the biggest reaction cross sections, because its selfenergy has also the largest imaginary part among all models considered (see Fig. 1 of Ref. [10]). Thus one can differentiate two sets of models, i.e, 2DD and IA selfenergies from THPH and IAPH ones. Besides, measurements, with precisions of about 10%, of the reaction cross sections would disentangle between THPH and IAPH models.

Let us look now to the experimental data. There only exist data [15] on K^- differential elastic cross sections for $q_{\mathrm{lab}} = 800$ MeV and from ^{12}C and ^{40}Ca. In Fig. 2 we compare the IA predictions (solid line), including up to $f-$waves (from Ref. [16]), to data. There also exist some data on total cross sections (mb), 338 ± 8 [306 ± 8], [18] from ^{12}C at $q_{\mathrm{lab}} = 800$ [655] MeV. The $\mathrm{IA}_{s+p+d+f}$ model provides again an acceptable description: 345 mb at 800 MeV and 304 mb at 655 MeV. Thus, this region is less sensitive to in nuclear medium effects than the K^- atom one. Indeed, the Glauber approximation also describes the 800 MeV scattering data, as discussed in [17]. This work also corroborates that the imaginary part of the K^-N amplitude, obtained from the K^--nucleus scattering data, is close to that deduced in the vacuum. Besides, the contribution of d and f waves, not included in the THPH model, turn out to be important (compare the solid line to the IA results obtained when only s and p waves –dot-dashed line– are considered, in Fig. 2). In addition, the models of Refs. [2] and [11] for the s and p K^-N waves, though realistic near threshold, can not be safely extrapolated to momenta as high as 800 MeV. Thus, one expects the poor description of data provided by the THPH model. It is however surprising, that the IAPH predictions turn out to be almost indistinguishable from the $\mathrm{IA}_{s+p+d+f}$ ones. This is merely a coincidence and, it occurs since accidentally at this momentum, $b_0^{\mathrm{IA}}(\sqrt{s})$ is approximately equal to $\tilde{b}_0$.

To finish, we also present results at an intermediate K^- momentum ($q_{\mathrm{lab}} = 300$ MeV), despite the fact that

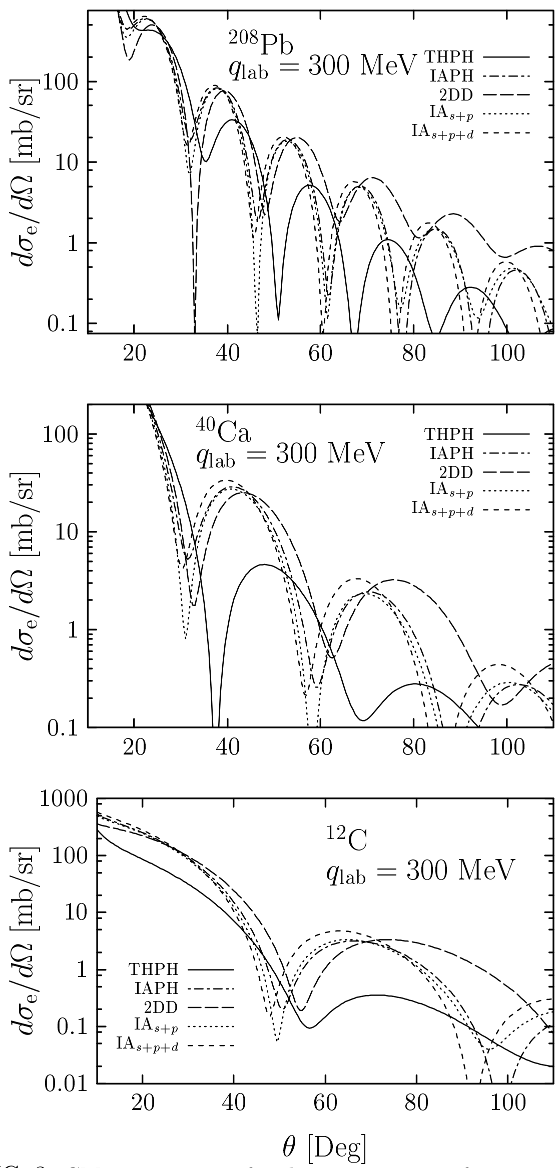

FIG. 3: CM cross sections for elastic scattering of $q_{\rm lab} = 300$ MeV K^- from ^{12}C, ^{40}Ca and ^{208}Pb with different K^- selfenergies.

there exist no data. For this momentum, calculations based on the IA shows that higher waves than the p one have a small/moderate contribution and therefore can be neglected in some approximations. Thus in Fig. 3 and bottom part of Table I, we compare again the THPH, 2DD and IAPH models for the K^- selfenergy inside the nuclear medium, together with the IA results including up to the p-wave, or up to the d-wave (partial waves are taken from Ref. [16]). The first observation is that the 2DD model differs now more than for the 127 MeV momentum case, from the IA models. This is mainly due to the effect of p-wave in the latter ones. The second observation is that the semiphenomenological model THPH leads to a pattern clearly different than the rest of selfenergies, not only for the elastic differential cross section but also in the integrated ones compiled in Table I. This is in principle good news, because then a scattering measurement in this region of K^- momentum will be definitive to disentangle between this approach and the others considered in Fig. 3 and bottom of Table I. However a word of caution must be said here, the s-wave part of the antikaon selfenergy of Ref. [5] is based on a model for the K^-N scattering in the free space that, though it is quite successful near threshold, predicts amplitudes for the isoscalar channel around $q_{\rm lab} = 300$ MeV, with real parts which are in total disagreement (in sign and in size, see Ref. [19]) with the analysis of Ref. [16]. Thus, most probably one cannot trust the THPH model to describe the K^--dynamics at this momentum. Indeed, there is no reason either to believe more in the 2DD and IAPH models, and we believe that the more reliable predictions for $q_{\rm lab} = 300$ MeV are those based on the IA.

Acknowledgments

We thank to E.Oset and A.Ramos for useful discussions. A.J.M. acknowledges a fellowship from the University of Granada. This work was supported by Junta de Andalucía, DGI and FEDER funds (BFM2002-03218).

[1] N. Kaiser, P.B. Siegel and W. Weise, Nucl. Phys. **A594** (1995) 325; *ibidem* Phys. Lett. **B362** (1995) 23.
[2] E. Oset and A. Ramos, Nucl. Phys. **A635** (1998) 99.
[3] J.A. Oller and U. Meißner, Phys. Lett. **B500** (2001) 263.
[4] C. García-Recio, J. Nieves, E. Ruiz Arriola and M.J. Vicente Vacas, hep-ph/0210311.
[5] A. Ramos and E. Oset, Nucl. Phys. **A671** (2000) 481.
[6] C.J.Batty, E. Friedman and A. Gal, Phys. Rep. **287** (1997) 385.
[7] E. Friedman, A. Gal and C.J. Batty, Phys. Lett. **B308** (1993) 6; *ibidem* Nucl.Phys.**A579** (1994) 518.
[8] E. Friedman and A. Gal, Phys.Lett. **B459** (1999) 43.
[9] S. Hirenzaki *et al.,* Phys. Rev. **C61** (2000) 055205.
[10] A. Baca, C. García-Recio and J. Nieves, Nucl. Phys. **A673** (2000) 335.
[11] C. García-Recio, J. Nieves, E. Oset and A. Ramos, Nucl. Phys. **A703** (2002) 271.
[12] D. Jido, E. Oset and A. Ramos, Phys. Rev. **C66** (2002) 055203.
[13] J. Nieves, E. Oset and C. García-Recio, Nucl. Phys. **A554** (1993) 509; *ibidem* Nucl. Phys. **A554** (1993) 554.
[14] A. D. Martin, Nucl. Phys. **B179** (1981) 33.
[15] D. Marlow, et al., Phys. Rev. **C25** (1982) 2619.
[16] G.P. Gopal et al., Nucl. Phys. **B119** (1977) 362.
[17] A. Sibirtsev and W. Cassing, Phys. Rev. **C61** (2000) 057601.
[18] D.V. Bugg, et al., Phys. Rev. **168** (1968) 1466.
[19] E. Oset, A. Ramos and C. Bennhold, Phys. Lett. **B522** (2002) 260.